Why one should use Youla-Kucera parametrization in adaptive feedforward noise attenuation?

Ioan Doré Landau, Tudor-Bogdan Airimitoaie, Raúl Meléndez, Luc Dugard

Why one should use Youla-Kucera parametrization in adaptive feeforward noise attenuation?

Ioan Doré Landau, Tudor-Bogdan Airimitoaie, Raul Melendez, and Luc Dugard

***Abstract*— A crucial problem in adaptive feedforward noise attenuation is the presence of an "internal" positive acoustical feedback between the compensation system and the reference source which is a cause of instabilities. Adaptive algorithms for feedforward active compensation having an infinite impulse response (IIR) or a finite impulse response (FIR) structure have been developed from a stability point of view. Nevertheless, in order to separate the problem of stabilizing the internal positive feedback loop from the minimization of the residual noise, the Youla–Kučera (YK) parametrization of the feedforward compensator has been proposed and algorithms have been developed from a stability point of view. Since the stability of the internal loop is a key issue in practice, the present paper using an unified presentation of the algorithms available discusses the stability conditions associated with the various algorithms and their properties. It is shown that the FIRYK configuration offers, from the stability point of view, the best option. Experimental results obtained on a relevant test-bench will illustrate the theoretical analysis.**

I. INTRODUCTION

Adaptive feedforward broad-band noise compensation is currently used when a correlated measurement with the disturbance (an image of the disturbance) is available. Most of the active feedforward noise control systems feature an internal "positive" acoustical feedback between the compensation system and the reference source (a correlated measurement with the disturbance). This internal positive feedback loop often leads to the instability of the system if it is not taken into account in the design stage ([1]).

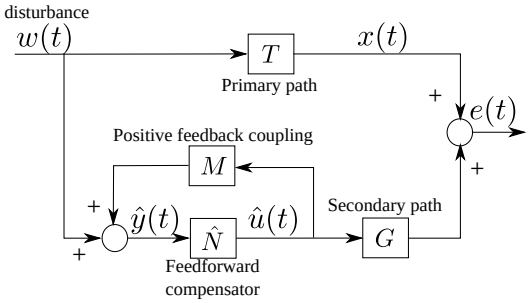

Fig. 1. Adaptive active noise feedforward compensation.

Figure 1 gives the basic block diagram of the adaptive feedforward compensation in the presence of the internal positive coupling between the output of the compensator and the measurement of the image of the incoming noise. The incoming noise propagates through the so called *primary path* and its effect is compensated through a secondary noise source (*secondary path*) driven by a feedforward compensator. The input to the feedforward compensator is the sum of the image of the incoming noise and of the internal acoustical positive feedback.

Single and multiple narrow-band disturbances can be efficiently attenuated by adaptive feedback configurations ([2], [3]). Nevertheless, the efficient use of the feedback approach for attenuation of broad-band noise is limited by the Bode integral. Therefore adaptive feedforward noise compensation is particularly dedicated to the attenuation of broad-band noise with unknown and time-varying characteristics.

Stability analysis of the adaptive feedforward compensation schemes taking into account the internal positive loop is an important aspect (see [4], [5], [6], [7], [8]). The stability analysis makes the assumption that there exists a compensator N such that the internal positive loop (formed by M and N in feedback) is stable and such that the perfect matching of the primary path is achieved.[1]

Starting with [6], a new approach emerged in the area of active noise and vibration control (ANVC), namely the design of the adaptation algorithms starting from a stability point of view and taking into account the internal positive feedback from the beginning. In the field of active vibration control (AVC), the paper [7] provides a full synthesis procedure for asymptotically stable adaptation algorithms using infinite impulse response (IIR) feedforard compensators in the presence of the internal feedback. These algorithms can be used also in active noise control (ANC) as it will be shown in this paper.

Since assuring the stability of the internal positive feedback loop is essential in applications, in [9] it is proposed to separate the stabilization of the internal positive feedback loop from the minimization of the residual noise by using a Youla–Kučera (YK) parametrization of the feedforward compensator. A tuning procedure based on system identification has been proposed and tested on a silencer. This idea has been used in [10] for developing direct adaptive feedforward compensation schemes using the YK parametrization of finite impulse response (FIR) or IIR form for the feedforward compensator. While these algorithms have been developped and tested in the context of AVC [8], they can be used also

The work of Raul Melendez was supported by Consejo Nacional de Ciencia y tecnología de México, CONACYT.

[1]Ioan Doré Landau, Raul Melendez, and Luc Dugard are with the Univ. Grenoble Alpes, CNRS, Grenoble INP, GIPSA-lab, 38000 Grenoble, France ioan-dore.landau; raul.melendez; luc.dugard@gipsa-lab.grenoble-inp.fr,

[2]Tudor-Bogdan Airimitoaie is with the Univ. Bordeaux, CNRS, Bordeaux INP, IMS, 33405 Talence, France tudor-bogdan.airimitoaie@u-bordeaux.fr

[1]This hypothesis of perfect matching of the primary path can be relaxed under certain conditions (see [7]).

in the field of ANC.

The various algorithms proposed for IIR or FIR compensators even if they assure the stability of the full system under some strictly positive real (SPR) conditions, they do not guarantee that the poles of the internal positive loop are not too close to the unit circle. One may ask if such a situation may occur. Considering the block diagram shown in Fig. 1. One can view this system as a Model Reference Adaptive System. In order to achieve perfect matching, the internal closed loop which is the effective feedforward compensator will try to cancel all the zeros of the secondary path which are not zeros of the primary path. This will imply that the poles of the internal closed loop will tend towards the zeros of the secondary path. Unfortunately, as it will be shown in the experimental section, the model of the secondary path in the context of noise attenuation in ducts (typical application field) have very low damped complex zeros. Therefore, as it will be shown, despite very good attenuation properties, the FIR (IIR) compensators will lead to the presence of closed-loop poles extremely close to the unit circle. So the problem of securing a disk of radius less than 1 is very important from a practical point of view, even if one has to accept slightly less good performances. YK parametrized adaptive feedforward compensators can offer such a solution. An FIRYK configuration will allow to define from the beginning the desired closed-loop poles (design of the central controller) and these poles will remain unchanged independently of the values of the parameters of the FIRYK filter.

The FIRYK configuration offers also another advantage: by an appropriate design of the central controller one can remove the SPR condition for stability (or more exactly, it will only depend on the precision of the estimation of the reverse path M, and current techniques of system identification extract excellent models from data).

There is also another advantage of using an FIRYK configuration. A necessary condition for perfect matching is that the transportation delay[2] of the secondary path should be smaller or equal than the transportation delay of the primary path. For most applications till recently, the design of the physical system has been done such that this constraint be satisfied. Nevertheless, there are potential application fields where, because of thermal constraints, this condition can not be fulfilled. It will be shown that despite the violation of the delay constraints the FIRYK can still operate with good performance while all the other configurations except the FIR are unstable (but the FIR gives poor performance).

The paper is organized as follows: in Section II, the various structures and algorithms will be presented under an unified form called "Generalized Youla-Kučera". Section III will examine comparatively various particular configurations and algorithms proposed in terms of stability conditions. Results obtained on an experimental test-bench (a core of a duct silencer) will illustrate some important properties of the algorithms in Section IV.

II. Basic Equations and Notations

The block diagram associated with an adaptive feeforward compensator using a generalized Youla-Kučera structure for adaptive feedforward compensators is shown in Fig. 2.

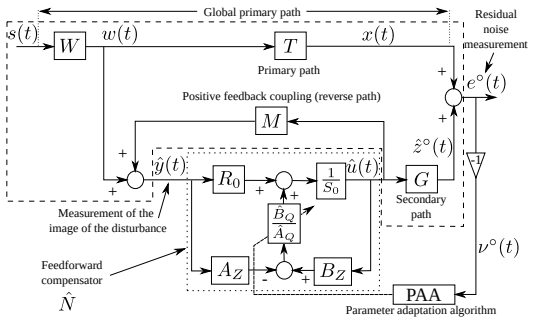

Fig. 2. Adaptive feedforward disturbance compensation using the generalized Youla–Kučera parametrization.

The primary (T), secondary (G), and reverse (positive coupling) (M) paths represented in Fig. 2 are characterized by the asymptotically stable transfer operators:

$$X(q^{-1}) = \frac{B_X(q^{-1})}{A_X(q^{-1})} = \frac{b_1^X q^{-1} + ... + b_{n_{B_X}}^X q^{-n_{B_X}}}{1 + a_1^X q^{-1} + ... + a_{n_{A_X}}^X q^{-n_{A_X}}}, \tag{1}$$

with $B_X = q^{-1} B_X^*$ for any $X \in \{D, G, M\}$. $\hat{G} = \frac{\hat{B}_G}{\hat{A}_G}$, $\hat{M} = \frac{\hat{B}_M}{\hat{A}_M}$, and $\hat{D} = \frac{\hat{B}_D}{\hat{A}_D}$ denote the identified (estimated) models of G, M, and D.

Polynomials A_Z and B_Z are defined as:

$$A_Z = a_0^Z + a_1^Z q^{-1} + ... \tag{2}$$

$$B_Z = b_1^Z q^{-1} + ... \tag{3}$$

The optimal feedforward compensator which will minimize the residual noise can be write as:

$$N = \frac{R}{S} = \frac{A_Q R_0 - B_Q A_Z}{A_Q S_0 - B_Q B_Z} \tag{4}$$

where the optimal filter $Q(q^{-1})$ has an IIR structure

$$Q = \frac{B_Q}{A_Q} = \frac{b_0^Q + b_1^Q q^{-1} + \ldots + b_{n_{B_Q}}^Q q^{-n_{B_Q}}}{1 + a_1^Q q^{-1} + \ldots + a_{n_{A_Q}}^Q q^{-n_{A_Q}}} \tag{5}$$

and $R_0(q^{-1})$, $S_0(q^{-1}) = 1 + q^{-1} S_0^*(q^{-1})$ are the polynomials of the central (stabilizing) filter and $A_Z(q^{-1})$, $B_Z(q^{-1})$ are given in (2) and (3)[3].

The estimated QIIR filter is denoted by $\hat{Q}(q^{-1})$ or $\hat{Q}(\hat{\theta}, q^{-1})$ when it is a linear filter with constant coefficients or $\hat{Q}(t, q^{-1})$ during estimation (adaptation). The vector of parameters of the optimal QIIR filter assuring perfect matching will be denoted by

$$\theta^T = [b_0^Q, \ldots, b_{n_{B_Q}}^Q, a_1^Q, \ldots, a_{n_{A_Q}}^Q] = [\theta_{B_Q}^T, \theta_{A_Q}^T]. \tag{6}$$

[2]The transportation delay is directly related to the speed of the sound and the geometry of the system.

[3]The following notation for polynomials will be used throughout this paper: $A(q^{-1}) = a_0 + \sum_{i=1}^{n_A} a_i q^{-i} = a_0 + q^{-1} A^*(q^{-1})$.

The vector of parameters for the estimated $\hat{Q}$IIR filter

$$\hat{Q}(q^{-1}) = \frac{\hat{B}_Q(q^{-1})}{\hat{A}_Q(q^{-1})} = \frac{\hat{b}_0^Q + \hat{b}_1^Q q^{-1} + \ldots + \hat{b}_{n_{B_Q}}^Q q^{-n_{B_Q}}}{1 + \hat{a}_1^Q q^{-1} + \ldots + \hat{a}_{n_{A_Q}}^Q q^{-n_{A_Q}}} \tag{7}$$

is denoted by

$$\hat{\theta}^T = [\hat{b}_0^Q, \ldots, \hat{b}_{n_{B_Q}}^Q, \hat{a}_1^Q, \ldots, \hat{a}_{n_{A_Q}}^Q] = [\hat{\theta}_{B_Q}^T, \hat{\theta}_{A_Q}^T]. \tag{8}$$

The input of the feedforward filter (called also reference) is denoted by $\hat{y}(t)$ and it corresponds to the measurement provided by the primary microphone. In the absence of the compensation loop (open-loop operation) $\hat{y}(t) = w(t)$. The output of the feedforward compensator (which is the control signal applied to the secondary path) is denoted by $\hat{u}(t+1) = \hat{u}(t+1/\hat{\theta}(t+1))$ (*a posteriori* output).

The *a priori* output of the estimated feedforward compensator using an IIRYK parametrization for the case of time-varying parameter estimates is given by (using (4))

$$\begin{aligned}\hat{u}^\circ(t+1) &= \hat{u}(t+1|\hat{\theta}(t)) \\ &= -\hat{S}^*(t,q^{-1})\hat{u}(t) + \hat{R}(t,q^{-1})\hat{y}(t+1) \\ &= -S_0^*\hat{u}(t) + R_0\hat{y}(t+1) - \hat{A}_Q(t,q^{-1})^*\beta(t) \\ &\quad + \hat{B}_Q(t,q^{-1})\alpha(t+1),\end{aligned} \tag{9}$$

and

$$\begin{aligned}\hat{u}(t+1) = -S_0^*\hat{u}(t) + R_0\hat{y}(t+1) - \hat{A}_Q(t+1,q^{-1})^*\beta(t) \\ + \hat{B}_Q(t+1,q^{-1})\alpha(t+1),\end{aligned} \tag{10}$$

where $\beta(t) = S_0\hat{u}(t) - R_0\hat{y}(t)$ (see also Fig. 2).

The objective is to develop stable recursive algorithms for adaptation of the parameters of the Q filter such that the measured residual error (noise in ANC) be minimized in the sense of a certain criterion. This has to be done for broad-band disturbances $w(t)$ (or $s(t)$) with unknown and variable spectral characteristics and an unknown primary path model.

The algorithms for adaptive feedforward compensation have been developed under the following basic hypotheses

1) (Perfect matching condition) There exists a value of the Q parameters such that
$$\frac{G \cdot A_M(R_0A_Q - A_ZB_Q)}{A_Q(A_MS_0 - B_MR_0) - B_Q(B_ZA_M - B_MA_Z)} = -T.$$
2) The characteristic polynomial of the internal closed-loop for $A_Q = 1$ and $B_Q = 0$
$$P_0(z^{-1}) = A_M(z^{-1})S_0(z^{-1}) - B_M(z^{-1})R_0(z^{-1})$$
is a Hurwitz polynomial.
3) (Stability of the internal loop) The characteristic polynomial of the internal closed-loop for the values of A_Q and B_Q assuring perfect matching is a Hurwitz polynomial:
$$P = A_Q(A_MS_0 - B_MR_0) - B_Q(B_ZA_M - B_MA_Z)$$

A first step in the development of the algorithms is to establish for a fixed estimated compensator a relation between the error on the Q-parameters (with respect to the optimal values) and the adaptation error ν. This is summarized in the following lemma.

Lemma 1: Under the hypothesis 1–3 for the system described by eqs. (1)–(10) using an estimated generalized Youla-Kučera parameterized feedforward compensator with constant parameters, one has:

$$\nu(t+1/\hat{\theta}) = \frac{A_MG}{A_QP_0 - B_Q(B_ZA_M - B_MA_Z)}[\theta - \hat{\theta}]^T\phi(t), \tag{11}$$

with $\phi(t)$ given by:

$$\begin{aligned}\phi^T(t) = [\alpha(t+1), \alpha(t), \ldots, \alpha(t - n_{B_Q} + 1), \\ - \beta(t), -\beta(t-1), \ldots, -\beta(t - n_{A_Q})].\end{aligned} \tag{12}$$

where:

$$\begin{aligned}\alpha(t+1) &= B_M\hat{u}(t+1) - A_M\hat{y}(t+1) = \\ &= B_M^*\hat{u}(t) - A_M\hat{y}(t+1) \qquad (13a) \\ \beta(t) &= S_0\hat{u}(t) - R_0\hat{y}(t). \qquad (13b)\end{aligned}$$

The proof of this lemma follows the proof given in Appendix A of [10] with the appropriate change of notations and is omitted.

For assuring the stability of the system one needs to filter the observation vector $\phi(t)$. Filtering the vector $\phi(t)$ through an asymptotically stable filter $L(q^{-1}) = \frac{B_L}{A_L}$, (11) for $\hat{\theta} = constant$ becomes

$$\begin{aligned}\nu(t+1/\hat{\theta}) = \frac{A_MG}{(A_QP_0 - B_Q(B_ZA_M - B_MA_Z))\,L} \cdot \\ \cdot [\theta - \hat{\theta}]^T\phi_f(t)\end{aligned} \tag{14}$$

with

$$\begin{aligned}\phi_f(t) = L(q^{-1})\phi(t) = [\alpha_f(t+1), \ldots, \alpha_f(t - n_{B_Q} + 1), \\ \beta_f(t), \beta_f(t-1), \ldots, \beta_f(t - n_{A_Q})]\end{aligned} \tag{15}$$

where

$$\alpha_f(t+1) = L(q^{-1})\alpha(t+1),\ \beta_f(t) = L(q^{-1})\beta(t). \tag{16}$$

When the parameters of $\hat{Q}$ evolve over time and neglecting the non-commutativity of the time-varying operators, (14) transforms into[4]

$$\begin{aligned}\nu(t+1/\hat{\theta}(t+1)) = \frac{A_MG}{[A_QP_0 - B_Q(B_ZA_M - B_MA_Z)]L} \cdot \\ \cdot [\theta - \hat{\theta}(t+1)]^T\phi_f(t).\end{aligned} \tag{17}$$

Equation (17) has the standard form for an *a posteriori* adaptation error ([11]), which immediately suggests to use

[4]Nevertheless, exact algorithms can be developed taking into account the non-commutativity of the time varying operators - see [11].

the following parameter adaptation algorithm (PAA):

$$\hat{\theta}(t+1) = \hat{\theta}(t) + F(t)\psi(t)\nu(t+1)\ ; \tag{18a}$$

$$\nu(t+1) = \frac{\nu^0(t+1)}{1+\psi^T(t)F(t)\psi(t)}\ ; \tag{18b}$$

$$F(t+1) = \frac{1}{\lambda_1(t)}\left[F(t) - \frac{F(t)\psi(t)\psi^T(t)F(t)}{\frac{\lambda_1(t)}{\lambda_2(t)} + \psi^T(t)F(t)\psi(t)}\right] \tag{18c}$$

$$1 \geq \lambda_1(t) > 0; 0 \leq \lambda_2(t) < 2; F(0) > 0 \tag{18d}$$

$$\psi(t) = \phi_f(t), \tag{18e}$$

where $\lambda_1(t)$ and $\lambda_2(t)$ allow to obtain various profiles for the matrix adaptation gain $F(t)$ (see [11]). By taking $\lambda_2(t) \equiv 0$ and $\lambda_1(t) \equiv 1$, one gets a constant adaptation gain matrix. Choosing $F = \gamma I$, $\gamma > 0$ one gets a scalar adaptation gain. The equation (18a) for updating the parameter vector becomes:

$$\hat{\theta}(t+1) = \hat{\theta}(t) + \gamma\Phi(t)\frac{\nu^\circ(t+1)}{1+\gamma\Phi^T(t)\Phi(t)}. \tag{19}$$

III. Specific Cases

1) For $A_Z = -1$, $B_Z = 0$, $R_0 = 0$, $S_0 = 1$: we are in the context of IIR (FIR) adaptive feedforward compensators discusssed in [7]. In this context there are two basic algorithms:
FUPLR (Filtered-U pseudo linear regression): $L = \hat{G}$ and
FUSBA (Filtered-U stability based algorithm): $L = \frac{\hat{A}_M}{\hat{P}}\hat{G}$, with $\hat{P} = \hat{A}_M\hat{S} - \hat{B}_M\hat{R}$.

The stability condition for FUPLR is: $\frac{A_M G}{P\hat{G}} - \frac{\lambda}{2} = SPR$ with $\lambda = \max\lambda_2(t)$ and for the FUSBA the stability condition is: $\frac{A_M\hat{P}G}{\hat{A}_M P\hat{G}} - \frac{\lambda}{2} = SPR \quad (\lambda = \max\lambda_2(t))$. For the FUSBA algorithm, the SPR condition is milder. Note that the FUSBA algorithm requires initialization over a certain horizon using FUPLR. This implies that the SPR condition for FUPLR is fulfilled at least in the average [12], [7]. Note that the stability conditions for FUPLR is "global" while for the FUSBA is "local" (one implicitly assumes that the FUPLR algorithm brings the parameters in the vicinity of the equilibrium point).

2) For $A_Z = A_M$, $B_Z = B_M$: we are in the context of the IIRYK feedforward compensator which has been discussed in [10]. In this context one has two basic algorithms:
FUPLR: $L = \hat{G}$ and
FUSBA: $L = \frac{\hat{A}_M}{\hat{P}}\hat{G}$, where $\hat{P} = \hat{A}_Q(A_M S_0 - B_M R_0)$. The stability condition associated to the FUPLR is that $\frac{A_M G}{P\hat{G}} - \frac{\lambda}{2} = SPR \quad (\lambda = \max\lambda_2(t))$ and the stability condition associated with th FUSBA is that: $\frac{A_M\hat{P}G}{\hat{A}_M P\hat{G}} - \frac{\lambda}{2} = SPR \quad (\lambda = \max\lambda_2(t))$.

In this case also the FUSBA algorithm requires initialization using the FUPLR algorithm.[5] This implies that the SPR condition for the FUPLR is satisfied at least on the average. The FUPLR stability condition is "global" while the FUSBA condition is "local".

[5]Or with an approximated FUSBA algorithm (using the filter $L = \frac{A_M}{P_0}\hat{G}$).

3) For $A_Z = A_M$, $B_Z = B_M$, $A_Q = 1$: we are in the context of the FIRYK feedforward compensator (see [10]). One can consider two adaptation algorithms:
FUPLR: $L = \hat{G}$ and
FUSBA: $L = \frac{\hat{A}_M}{\hat{P}_0}\hat{G}$, where $\hat{P}_0 = (\hat{A}_M S_0 - \hat{B}_M R_0)$.

The stability condition associated with the FUPLR is that: $\frac{A_M G}{P_0\hat{G}} - \frac{\lambda}{2} = SPR \quad (\lambda = \max\lambda_2(t))$. The stability condition associated with the FUSBA is that: $\frac{A_M\hat{P}_0 G}{\hat{A}_M P_0\hat{G}} - \frac{\lambda}{2} = SPR \quad (\lambda = \max\lambda_2(t))$. In this case for both FUPLR and FUSBA the stability conditions are "global". The main difference with respect to the previous cases is twofold:

- The FUSBA algorithm can be implemented from the beginning since P_0 is known and constant and the stability condition is global.
- The design of the central controller can be used for fulfilling the SPR conditions.[6]

If the central controller is designed such that $\hat{P}_0 = \hat{A}_M$, then FUPLR and FUSBA are almost the same and the fulfillment of the SPR condition will depend only on the quality of the estimation of the transfer M. This is a key point because not only the stability of the internal loop will be assured for any finite value of the parameters of the FIR Youla-Kučera filter but in addition the system will be operated under a global stability condition easy to fulfill and allowing to use high values of the adaptation gain leading to fast adaptation.

A consequence of this property is that the YKFIR configuration can be safely used even if the perfect matching condition is not fulfilled. Such a situation occurs in practice when the pure delay (propagation delay) on the secondary path is larger than the pure delay of the primary path. This will be illustrated in the experimental results section.

For all the configurations scalar adaptation gains can also be used. The same filter L is used and the algorithms corresponding to FUPLR and FUSBA are termed: NFULMS[7] and SFUSBA respectively. The stability conditions are the same as for the matrix case except that in this case $\lambda = 0$.

Youla–Kučera Parametrization—Some Remarks

Two major observations when using the Youla–Kučera parametrization have to be made:

- If an FIR Q filter is used, the poles of the internal closed-loop will be defined by the central compensator R_0, S_0 and they will remain unchanged independently of the values of the parameters of the Q filter. The stability condition for the FUSBA algorithm is global.
- If an IIR Q filter is used, the poles of the internal closed-loop will be defined by the central compensator but additional poles corresponding to the denominator of the Q filter will be added. The stability condition for the FUSBA algorithm is local and an initialization with the FUPLR algorithm is necessary.

[6]The main objective of the central controller is to stabilize the internal loop.

[7]For the case of FIR and IIR structures the FXLMS and respectively the FULMS can be interpreted as approximations of the NFULMS algorithm.

IV. Experimental Results

The core of a noise silencer is used as a test bench. Two configurations have been considered: Configuration A shown in Fig. 3 (the pure delay of the secondary path is smaller than the pure delay of the primary path) and configuration B shown in Fig. 4 (the pure delay of the secondary path is larger than the pure delay of the primary path).

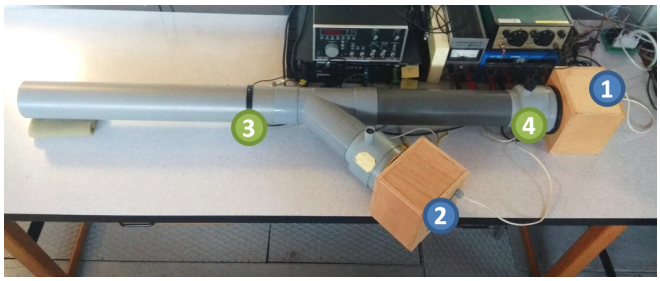

Fig. 3. Duct active noise control test-bench. Configuration A (Photo).

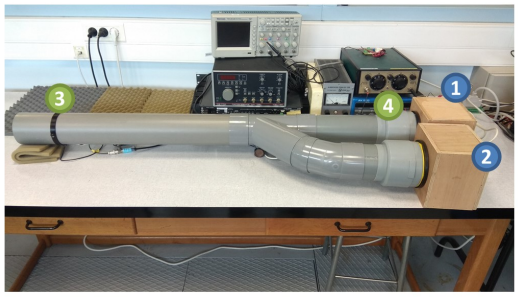

Fig. 4. Duct active noise control test-bench. Configuration B (Photo).

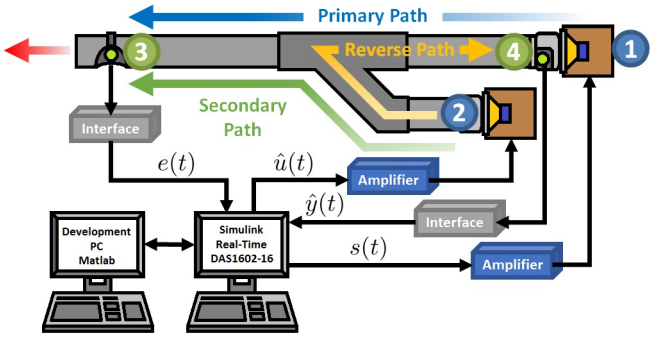

Fig. 5. Duct active noise control test-bench diagram.

Figure 5 gives the block diagram of the system. The speaker used as the source of disturbances is labeled as 1, while the control speaker is marked as 2. At the pipe's open end, the microphone that measures the system's output (residual noise $e(t)$) is denoted as 3. Inside the pipe, close to the source of disturbances, the second microphone, labeled as 4, measures the image of the incoming noise, denoted as $\hat{y}(t)$. The various paths are indicated on the figure. The system is connected to an xPC Target computer with Simulink Real-time® environment. The sampling frequency is $f_s = 2500$ Hz. The various paths have been identified by standard experimental identification techniques which are described in [13]. The various paths' models are characterized by the presence of multiple very low damped complex poles and complex zeros. The orders for the various models are summarized in Table I for configurations A and B.

Config.	A	A	A	B	B	B
Model	n_B	n_A	d	n_B	n_A	d
Primary (global)	20	24	7	20	27	8
Secondary	27	26	6	20	27	9
Reverse	22	25	5	33	33	4

TABLE I

Orders of the identified system paths.Configuration A and B.

1) Configuration A: The objective is to illustrate first the properties of the FIRYK configuration and the importance of the design of the central controller for the fulfillment of the SPR condition for stability. In the first design, the central controller introduces some attenuation in the region of operation (70 to 270 Hz). In the second design, the central controller was computed such that $P_0 = \hat{A}_M$ without introducing attenuation. Table II gives the results obtained using the two different central controllers with 60 adapted parameters. In the case $P_0 \neq \hat{A}_M$, the FUPLR algorithm

Cl. Poles	$P_0 \neq \hat{A}_M$	$P_0 = \hat{A}_M$
Adaptation algorithm	Atten. [dB]	Atten. [dB]
Matrix (FUSBA)	27.0	27.3
Matrix (FUPLR)	unstable	27.2
Scalar (SFUSBA)	26.7	27.1
Scalar (SFUPLR)	unstable	27.2

TABLE II

Experimental results for FIRYK 60/0 adaptive compensators using various adaptation algorithms (70-270 Hz broad-band disturbance, 180 s experiments).

is unstable. This can be easily understood by looking to the phase of the estimated transfer function $\frac{\hat{A}_M}{P_0}$ shown in Fig. 6 (obtained when using the FUSBA algorithm). Since the noise to be attenuated has an almost flat power spectral density (PSD) between 70 and 270 Hz, it is clear that the SPR condition is violated in a too large frequency spectrum (even using averaging arguments). By using the second design, for both FUPLR and FUSBA, the SPR condition will be the same and both algorithms will be stable and will provide identical performances as illustrated in Table II.

Figure 7 shows the PSD in open loop and in the presence of the FIRYK compensator[8]. As it can be seen, there is no significant amplification at the frequencies outside the attenuation zone. The estimation of the output sensitivity function of the internal loop for the FIRYK 60/0 using the FUSBA algorithm shows a maximum below 10 dB (modulus margin greater than 0.3). Figure 8 shows the PSD of an FIR and of an IIR adaptive compensator. Despite the fact that they assure a better attenuation in the region

[8]The number of the parameters of the compensator is denoted by nb/na (nb for the numerator, nb for the denominator)

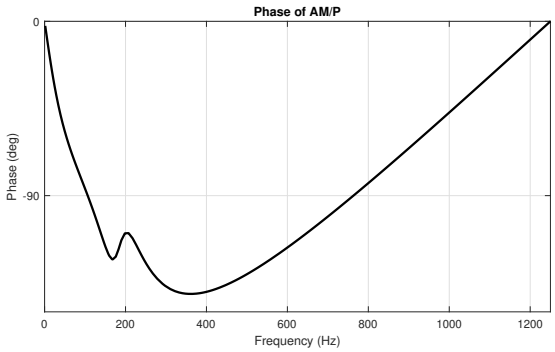

Fig. 6. Phase of $\frac{\hat{A}_M}{P}$ for the FIRYK 60/0 adaptive compensator (70-270 Hz disturbance, 600 s experiments).

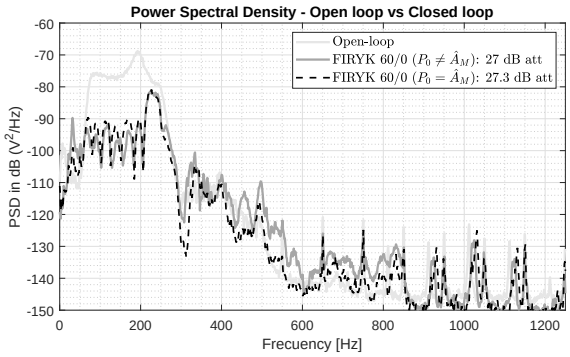

Fig. 7. PSD of the FIRYK 60/0 adaptive compensators using FUSBA matrix adaptation (70-270 Hz disturbance, 600 s experiments).

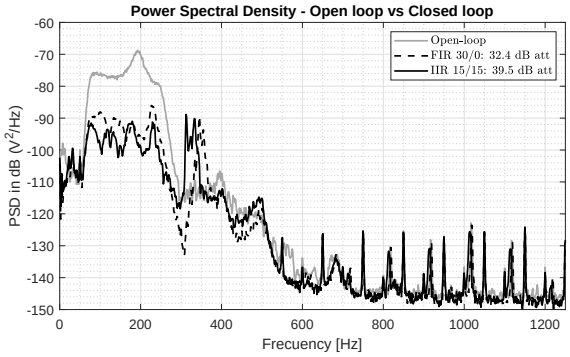

Fig. 8. PSD comparison of FIR 30/0 and IIR 15/15 standard adaptive compensators using FUSBA matrix adaptation (70-270 Hz disturbance, 600 s experiments).

70-270 Hz there is a very strong amplification outside the attenuation zone indicating the presence of a pair of very low damped complex poles (in the region around 320 Hz). Further analysis shows for the IIR configuration that the estimated output sensitivity function has a maximum of 26 dB in this region corresponding to a modulus margin of less than 0.06 (extremely close to instability).

2) Configuration B: In this configuration, all compensators are unstable except the FIR and the FIRYK. Figure 9 shows the PSD of the residual noise obtained over an horizon of 800 s for the FIR and the FIRYK compensators. Clearly the FIRYK compensator offers much better results in terms of attenuation (20.6 dB versus 10.4 dB for a noise covering the range 150-350 Hz).

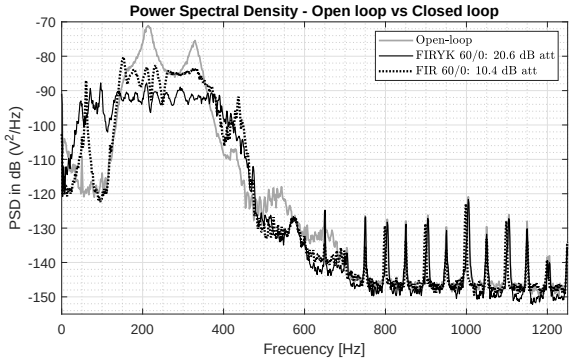

Fig. 9. PSD of the FIR and the FIRYK adaptive compensators using FUSBA (60 parameters, 150-350 Hz disturbance, 800 s experiments).

V. Concluding remark

In summary one can say that the FIRYK adaptive feedforward compensator offers a robust solution (with respect to the risk of instability of the internal loop) for adaptive feedforward noise attenuation.

References

[1] M. Bai and H. Lin, "Comparison of active noise control structures in the presence of acoustical feedback by using the H_∞ synthesis technique," *J. of Sound and Vibration*, vol. 206, pp. 453–471, 1997.

[2] F. Ben Amara, P. Kabamba, and A. Ulsoy, "Adaptive sinusoidal disturbance rejection in linear discrete-time systems - Part II: Experiments," *Journal of Dynamic Systems Measurement and Control*, vol. 121, pp. 655–659, 1999.

[3] I. D. Landau, M. R., D. L., and B. G., "Robust and adaptive feedback noise attenuation in ducts," *IEEE Transactions on Control System Technology*, vol. 24, no. 12, pp. 1–8, December 2017.

[4] A. Wang and W. Ren, "Convergence analysis of the Filtered-U algorithm for active noise control," *Signal Processing*, vol. 83, pp. 1239–1254, 1999.

[5] R. Fraanje, M. Verhaegen, and N. Doelman, "Convergence analysis of the Filtered-U LMS algorithm for active noise control in case perfect cancellation is not possible," *Signal Processing*, vol. 73, pp. 255–266, 2003.

[6] C. Jacobson, J. Johnson, C.R., D. McCormick, and W. Sethares, "Stability of active noise control algorithms," *Signal Processing Letters, IEEE*, vol. 8, no. 3, pp. 74 –76, mar 2001.

[7] I. Landau, M. Alma, and T. Airimitoaie, "Adaptive feedforward compensation algorithms for active vibration control with mechanical coupling," *Automatica*, vol. 47, no. 10, pp. 2185 – 2196, 2011.

[8] I. D. Landau, T.-B. Airimitoaie, A. Castellanos Silva, and A. Constantinescu, *Adaptive and Robust Active Vibration Control—Methodology and Tests*, ser. Advances in Industrial Control. Springer Verlag, 2017.

[9] J. Zeng and R. de Callafon, "Recursive filter estimation for feedforward noise cancellation with acoustic coupling," *Journal of Sound and Vibration*, vol. 291, no. 3-5, pp. 1061 – 1079, 2006.

[10] I. D. Landau, T.-B. Airimitoaie, and M. Alma, "IIR Youla–Kučera parameterized adaptive feedforward compensators for active vibration control with mechanical coupling," *IEEE Transactions on Control System Technology*, vol. 21, no. 3, pp. 765–779, May 2013.

[11] I. D. Landau, R. Lozano, M. M'Saad, and A. Karimi, *Adaptive control*, 2nd ed. London: Springer, 2011.

[12] B. Anderson, R. Bitmead, C. Johnson, P. Kokotovic, R. Kosut, I. Mareels, L. Praly, and B. Riedle, *Stability of adaptive systems*. Cambridge Massachusetts , London, England: The M.I.T Press, 1986.

[13] R. Melendez, I. Landau, L. Dugard, and G. Buche, "Data driven design of tonal noise feedback cancellers," in *Proceedings of the 20th IFAC World Congress, Toulouse, France*, 2017, pp. 916–921.